THE JOURNAL OF PHYSICAL CHEMISTRY A

Article

Cite This: J. Phys. Chem. A 2018, 122, 6491−6499

pubs.acs.org/JPCA

Quantum-State-Selected Integral Cross Sections and Branching Ratios for the Ion−Molecule Reaction of $N_2^+(X^2\Sigma_g^+: \nu^+ = 0-2) + C_2H_4$ in the Collision Energy Range of 0.05−10.00 eV

Published as part of The Journal of Physical Chemistry virtual special issue "William M. Jackson Festschrift".

Yuntao Xu, Bo Xiong, Yih Chung Chang, and Cheuk-Yiu Ng*

Department of Chemistry, University of California, Davis, Davis, California 95616, United States

ABSTRACT: By implementing a vacuum ultraviolet laser-pulsed field ionization-photoion ion source with a double quadrupole−double octopole ion guide mass filter, we have obtained detailed quantum-vibrational-state-selected integral cross sections $\sigma_{\nu+}$, $\nu^+ = 0-2$, for the ion−molecule reaction of $N_2^+(X^2\Sigma_g^+: \nu^+ = 0-2) + C_2H_4$ in the center-of-mass kinetic energy range of $E_{cm} = 0.05-10.00$ eV. Three primary product channels corresponding to the formation of $C_2H_3^+$, $C_2H_2^+$, and N_2H^+ ions are identified with their $\sigma_{\nu+}$ values in the order of $\sigma_{\nu+}(C_2H_3^+) > \sigma_{\nu+}(C_2H_2^+) > \sigma_{\nu+}(N_2H^+)$. The minor $\sigma_{\nu+}(N_2H^+)$ channel is strongly inhibited by E_{cm} and observed only at $E_{cm} < 0.70$ eV. The high $\sigma_{\nu+}(C_2H_3^+)$ and $\sigma_{\nu+}(C_2H_2^+)$ values indicate that $C_2H_3^+$ and $C_2H_2^+$ product ions are formed by prompt dissociation of internally excited $C_2H_4^+$ ($C_2H_4^{+*}$) intermediates produced via the near-energy-resonance charge-transfer mechanism. The $\sigma_{\nu+}(C_2H_3^+)$ and $\sigma_{\nu+}(C_2H_2^+)$ are found to drop only mildly or stay nearly constant as a function of E_{cm} in the range of 0.05−6.00 eV. This observation is contrary to the expectation of a steep decline for the $\sigma_{\nu+}$ value commonly observed for an exothermic reaction pathway as E_{cm} is increased. Significant vibrational enhancement is observed for the $\sigma_{\nu+}(C_2H_3^+)$ and $\sigma_{\nu+}(C_2H_2^+)$ at $\nu^+ = 2$ and in the E_{cm} range of ∼0.20−7.00 eV. The branching ratios $\sigma_{\nu+}(C_2H_3^+):\sigma_{\nu+}(C_2H_2^+):\sigma_{\nu+}(N_2H^+)$ are also determined with high precision by measuring the intensities of product $C_2H_3^+$, $C_2H_2^+$, and N_2H^+ ions simultaneously at fixed E_{cm} values. The $\sigma_{\nu+}$ and branching ratio values reported here are useful contributions to the database needed for realistic modeling of the chemical compositions and evolutions of planetary atmospheres, such as the ionosphere of Titian. The quantum-state-selective results can also serve as experimental benchmarks for theoretical calculations on fundamental chemical reaction dynamics.

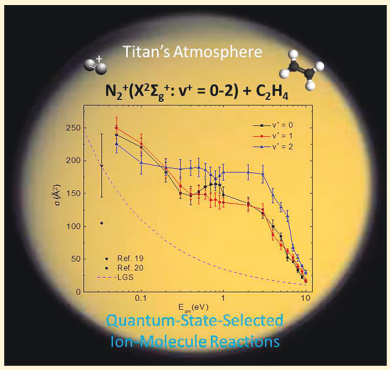

1. INTRODUCTION

Gaseous ion−molecule reactions play an important role in many gaseous chemical and physical environments, including interstellar clouds,[1,2] cometary comae,[3,4] terrestrial atmospheres,[5] combustion flames,[6] and plasma discharges.[7] It is recognized that an understanding of the chemical compositions and the evolutions of the chemical compositions in these environments requires detailed chemical modeling. However, because accurate reaction rate constants (k_r's), integral cross sections (σ's), and product branching ratios (BRs) for relevant ion−molecule reactions are mostly unavailable, reliable laboratory measurements are thus required to establish the database needed for the modeling effort. This work is concerned with σ and BR measurements for the quantum-vibrational-state-selected ion−molecule reaction $N_2^+(X^2\Sigma_g^+: \nu^+ = 0-2) + C_2H_4$ and can be considered as a continuation of our recent experimental investigations of the reactions between $N_2^+(X^2\Sigma_g^+: \nu^+ = 0-2)$ and CH_4 (C_2H_2, H_2O).[8−10] These reactions are recognized as key steps for the ion−molecule reaction network proposed for simulating the chemical compositions of Titan's ionosphere.

Since its discovery in 1665 by Christiaan Huygens,[11] Titan, the largest moon of Saturn, has been an object of continuous curiosity and intrigue. First recognized in 1944,[12] its substantial atmosphere has been considered as having one of the richest atmospheric chemistries in the Solar system.[13−17] On the basis of in situ measurements[13,16] by the Voyager spacecraft in 1980s and the Huygens probe in 2005,[18] the N_2 molecule was determined as the dominant neutral species with about 94% abundance, and the other 6% is made up of trace compounds including CH_4, C_2H_2, C_2H_4, and other hydrocarbon molecules. It is well-known that N_2^+ ions in the ionosphere of Titian are formed by ionization of neutral N_2 molecules by solar vacuum ultraviolet (VUV) radiation, energetic particles, and cosmic rays; and thus, the resulting N_2^+ ions can be formed in a wide range of internal states. The interactions among these molecular species are believed to be the basis for the complex nitrogen-rich organic chemistry occurring in Titian's atmosphere.

Unraveling the chemical compositions and the evolution of the atmosphere of Titan requires detailed σ and BR measurements for the ion−molecule reactions between N_2^+

Received: May 14, 2018
Revised: July 22, 2018
Published: July 23, 2018

DOI: 10.1021/acs.jpca.8b04587
J. Phys. Chem. A 2018, 122, 6491−6499

ions and hydrocarbon molecules. Being a homonuclear diatomic molecule without a dipole moment, the radiative lifetimes of internally excited $N_2^+(X^2\Sigma_g^+: \nu^+, N^+)$ ions are long. This, together with the fact that the chemical reactivity of the $N_2^+(X^2\Sigma_g^+: \nu^+, N^+)$ ion depends on its quantum-rovibrational state, makes it necessary to take into account the center-of-mass kinetic energy (E_{cm}) as well as the quantum-vibrational-state effects on the $N_2^+(X^2\Sigma_g^+; \nu^+, N^+) + C_2H_4$ reaction in order to achieve reliable modeling of the chemistry occurring in the ionosphere of Titan. However, quantum-state-selected σ and BR data, such as those presented here for the title reaction covering a wide range of E_{cm}'s, have not been reported previously.

Compared with the $N_2^+(X^2\Sigma_g^+: \nu^+ = 0-2) + CH_4$ (C_2H_2, H_2O) reactions,[8−10] very few experimental studies[19−22] have been made on the reaction of $N_2^+ + C_2H_4$, and almost all of them are on reaction kinetics rather than dynamics measurements. In 1998, by using an ion cyclotron resonance mass spectrometer, McEwan et al.[19] reported a k_r value of 1.30×10^{-9} cm^3 s^{-1} for the $N_2^+ + C_2H_4$ reaction leading to the formation of five product ions of $C_2H_3^+$, $C_2H_2^+$, HNC^+, $HCNH^+$, and N_2H^+, with the corresponding intensity ratio or BR of 0.50:0.20:0.10:0.10:0.10 at room temperature (T = 300 K). The same group later employed the selected ion flow tube method and published an updated k_r value of 7×10^{-10} cm^3 s^{-1}. In the latter study,[20] only two product ions species $C_2H_3^+$ and $C_2H_2^+$ were observed with a corresponding branch ratio of 0.64:0.36. In 2011, Gichuhi et al.[21] reinvestigated the $N_2^+ + C_2H_4$ reaction in a supersonic beam using a velocity map imaging TOF mass spectrometer. Two product ions $C_2H_3^+$ and $C_2H_2^+$ were observed in the latter experiment, giving a BR of 0.74:0.26 at $T = 40 \pm 5$ K. Recently, this reaction system was reviewed by Dutuit et al.,[22] who recommended a k_r value of 1.30×10^{-9} cm^3 s^{-1} with ±15% uncertainty. Three product ion species $C_2H_3^+$, $C_2H_2^+$, and N_2H^+ were also recommended with a corresponding BR of 0.67:0.23:0.10. Comparing these results reveals large discrepancies for both product ion identification and product BR measurements in previous experimental studies. These discrepancies have partly motivated the present $\sigma_{\nu+}$ and BR measurements for the quantum-vibrational-state-selected ion−molecule reaction $N_2^+(X^2\Sigma_g^+: \nu^+ = 0-2) + C_2H_4$.

The development of quantum-state-selected ion−molecule reaction studies in the past decades has rendered a major platform for the investigation of the E_{cm} and the quantum-rovibronic-state effects on chemical reactivity[23−26] of ions. The most challenging task for these experiments is to prepare reactant ions into single quantum-rovibronic states and still maintain a sufficiently high intensity for the state-selected ions to undergo single-collision measurements.[27] Recently, we introduced a novel VUV laser pulsed field ionization-photoion (VUV-PFI-PI) ion source,[28,29] in which a sequence of pulsed electric fields is designed to cleanly separate the non-state-selected prompt ions from the state-selected VUV-PFI-PI ions. The high kinetic energy resolution achieved for the VUV-PFI-PIs has also made possible σ-measurements down to E_{cm} = 30−40 meV. Employing this VUV-PFI-PI technique, we have successfully prepared $N_2^+(X^2\Sigma_g^+: \nu^+ = 0-2, N^+)$, $H_2O^+(X^2B_1: \nu_1^+\nu_2^+\nu_3^+ = 000, 020, 100; N^+_{Ka+Kc+})$, $H_2^+(X^2\Sigma_g^+: \nu^+ = 1-3; N^+)$, $O_2^+(a^4\Pi_{u5/2,3/2,1/2,-1/2}: \nu^+ = 1-2; J^+)$, and $O_2^+(X^2\Pi_{g3/2,1/2}: \nu^+ = 22-23; J^+)$ ions into single rovibronic-quantum states.[28,30−32] By coupling this high-resolution VUV laser PFI-PI ion source with the double quadrupole−double octopole (DQDO) ion guide mass filter developed in our laboratory, we obtained detailed σ and product BR values for the reactions $N_2^+(X) + Ar$,[29] $N_2^+(X) + CH_4$,[8] $N_2^+(X) + C_2H_2$,[9] $N_2^+(X) + H_2O$,[10] $H_2O^+(X) + D_2/H_2/HD$,[33−35] $H_2O^+(X) + CO$,[36] $H_2^+(X) + Ne$,[31] $H_2O^+(X) + N_2$,[10] $O_2^+(X) + Ar$,[32] and $O_2^+(a) + Ar$,[32] covering the E_{cm} range of 0.03−10.00 eV. The σ and BR measurements reported here are aimed to provide reliable and relevant chemical dynamics data for establishing the database needed for chemical modeling of planetary atmospheres.[37−40]

2. EXPERIMENT

A detailed description of the VUV laser PFI-PI DQDO ion−molecule reaction apparatus and the procedures employed for the present experiment was reported in detail previously.[28,29] Briefly, the ion−molecule reaction apparatus consists of a VUV laser PFI-PI ion source coupled to a DQDO mass filter, which is equipped with a dual set of radio frequency (rf)-octopole ion guides.

The VUV laser radiation used in this work is generated by four-wave frequency mixing schemes using Kr gas as the nonlinear medium. Here, the VUV laser in the range of 125 500−130 200 cm^{-1} generated by sum-frequency ($2\omega_1 + \omega_2$) mixing is used, where ω_1 and ω_2 represent the outputs of the ultraviolet (UV) and visible (VIS) dye lasers, respectively. The second and third harmonic outputs of an identical Nd:YAG laser (Spectra-Physics, Model PRO-290) operated at 15 Hz are employed to pump the UV and VIS dye lasers, respectively. The two-photon frequency $2\omega_1$ matches the 4p → 5p resonance transition of the Kr atom, and the VIS ω_2 output is tuned in the range of 30 770−37 040 cm^{-1} to generate the VUV sum-frequencies required for the experiment.

The quantum-rovibrational state-selected $N_2^+(X^2\Sigma_g^+: \nu^+ = 0-2; N^+ = 0-9)$ reactant ions are produced by PFI-PI of excited $N_2^*(n)$ molecules in high-n Rydberg states, which are formed by VUV laser photoexcitation of N_2 in the form of a supersonic molecular beam. By employing the sequential electric field pulse scheme, we achieved PFI-PI energy resolution of 2−4 cm^{-1} (full width at half-maximum, fwhm), which is sufficient to resolve single rotational transitions to the $N^+ = 0-9$ states associated with the $N_2^+(X^2\Sigma_g^+: \nu^+ = 0-2)$ vibrational bands. Here, for each PFI-PI vibrational band, N_2^+ ions were prepared by setting the VUV laser frequency at the strongest rotational peak position, i.e., the Q-branch. Thus, the vibrationally selected $N_2^+(\nu^+ = 0-2)$ ions thus prepared are in a distribution of the $N^+ = 0-9$ rotational states.[29]

The key to achieve high kinetic energy resolution or a narrow laboratory kinetic energy spread (ΔE_{lab}) for the PFI-PIs is to turn off the PFI and ion extraction electric field pulse before the PFI-PIs exit the photoionization/photoexcitation (PI/PEX) region, such that all PFI-PIs gain the same linear momentum during the PFI and PFI-PI extraction processes. As a result, the $\Delta E_{lab} \approx \pm 30-50$ meV[28] achieved in this experiment is mostly limited by the supersonic cooling of the N_2 molecular beam. Because prompt ions formed by direct photoionization of N_2 have lower kinetic energies than that of the PFI-PIs due to application of the retarding electric field pulse in the beginning detection cycle, we are able to cleanly separate and reject all background prompt ions from state-selected VUV-PF-PIs by using a simple potential energy barrier downstream of the ion source. Thus, only N_2^+ PFI-PIs can enter the rf-octopole ion guide reaction gas cell, where the $N_2^+(X^2\Sigma_g^+; \nu^+ = 0-2) + C_2H_4$ reaction occurs.

DOI: 10.1021/acs.jpca.8b04587
J. Phys. Chem. A 2018, 122, 6491−6499

In the present experiment, the C_2H_4 pressure used in the gas cell was in the range of from 1.0×10^{-5} to 1.0×10^{-4} Torr as monitored by a MKS Baratron. When the C_2H_4 pressure was 1×10^{-4} Torr, the number density of C_2H_4 molecules (ρ) was about 3.5×10^{12} cm^{-3}. The gas cell effective length (l) was about 5.6 cm. Therefore, the number of collisions (n) per reactant N_2^+ ion could be estimated roughly by using formula $n = \rho l \sigma$. Given the above values of ρ and l, the single-collision condition ($n \leq 1$) is considered to be satisfied for $\sigma < 510$ Å^2. The reaction gas cell is situated between two rf-octopole ion guides, which are powered by the same rf power supply. A small dc electric field can be applied between the two rf-octopoles, such that slow product ions formed in the gas cell can be effectively extracted from the reaction gas cell. All product ions produced in the reaction gas cell, along with the attenuated N_2^+ reactant PFI-PIs, are guided into the product quadrupole mass filter (QMF) for mass and intensity measurements. Here, the E_{cm} is converted from the laboratory kinetic energy (E_{lab}) using the formula $E_{cm} = E_{lab}\,[M/(m^+ + M)]$, where m^+ and M represent the masses of the N_2^+ ion and the C_2H_4 molecule, respectively.

The σ values are calculated by using the formula $\sigma = [(kT)/(Pl)][\ln((I + i)/I)]$, where k is the Boltzmann constant; T and P stand for the temperature and the pressure of the neutral reactant in the reactant gas cell, respectively; l represents the effective length of the gas cell;[28,29] I is the intensity of the unreacted reactant N_2^+ ions; and i is the intensity of the product ions. The σ's determined in the present study are the average of at least six independent measurements. The run-to-run uncertainty is in the range of 5−15%. The error limits for absolute σ values are estimated to be 30%.[28,29]

As pointed out in previous studies,[9,33,35] in an ion beam gas cell study, such as this one, the thermal motions of neutral C_2H_4 molecules in the reaction gas cell can be the main contribution to the ΔE_{cm}, especially at the low E_{cm} range.[41] For the reaction $N_2^+ + C_2H_4$, the estimated uncertainties for E_{cm} = 0.05, 0.10, and 0.5 eV are 0.08, 0.12, and 0.26 eV, respectively. The ΔE_{cm} spread can have the effect of smoothening structures of the $\sigma_{\nu+}$ curves, but the general trends for the $\sigma_{\nu+}$ curves are not expected to be greatly affected.

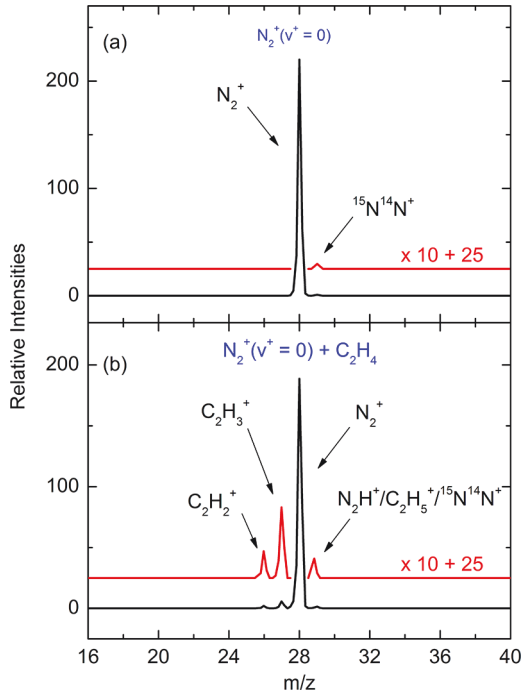

Figure 1. (a) Mass spectrum of reactant N_2^+ VUV-PFI-PI ions observed without filling the neutral reactant C_2H_4 gas in the rf-ion guide reaction gas cell. Besides the N_2^+ ion peak observed at m/z = 28, the minor ion peak for the isotopic molecules $^{15}N^{14}N^+$ at m/z = 29 is also evident, where the relative intensities for m/z = 28 and 29 are consistent with the natural abundances of $^{15}N/^{14}N$. (b) Mass spectrum recorded by filling the gas cell with C_2H_4 gas at a pressure of 1.0×10^{-4} Torr. In addition to N_2^+ and $^{15}N^{14}N^+$ ions, four more ion species are detected, which are $C_2H_2^+$, $C_2H_3^+$, N_2H^+, and $C_2H_5^+$. For both spectra of (a) and (b), the ion energy is set at E_{cm} = 0.10 eV.

3. RESULTS AND DISCUSSION

Mass Spectra. On the basis of previous studies,[22] the observation of product $C_2H_3^+$, $C_2H_2^+$, and N_2H^+ ions can be attributed to reactions 1−3, respectively. Assuming that previous studies of the $N_2^+ + C_2H_4$ reaction mostly involved the $N_2^+(X^2\Sigma_g^+;\ \nu^+ = 0)$ ground state, we have calculated the heats of reaction (ΔE's) for the three product channels as shown below.[42]

$$N_2^+(X^2\Sigma_g^+;\ \nu^+ = 0) + C_2H_4 \rightarrow C_2H_3^+ + N_2 + H \quad \Delta E = -2.378 \pm 0.006 \text{ eV} \tag{1}$$

$$\rightarrow C_2H_2^+ + N_2 + H_2 \quad \Delta E = -2.443 \pm 0.0030.009 \text{ eV} \tag{2}$$

$$\rightarrow N_2H^+ + C_2H_3 \quad \Delta E = -2.284 \pm 0.009 \text{ eV} \tag{3}$$

Reactions 1 and 2 can be rationalized to occur by a dissociative charge-transfer reaction mechanism, and reaction 3 can be ascribed to proceed via a H atom transfer pathway. All of these reactions are highly exothermic with exothermicities of >2.20 eV. The ΔE values for the $\nu^+ = 1$ and 2 vibrational states of N_2^+ can be obtained accordingly by using the known N_2^+ vibrational energy levels ($\nu^+ = 1$ and 2 vibrational states of N_2^+ are about 0.271 and 0.535 eV higher than that of the $\nu^+ = 0$ state, respectively).[29]

All these reaction channels are verified by the mass spectra observed at E_{cm} = 0.10 eV, as shown in Figure 1a,b. Figure 1a shows the mass spectrum of the N_2^+ PFI-PI ions (i.e., without neutral C_2H_4 filled in the reaction gas cell), and Figure 1b depicts the mass spectrum for the reaction of $N_2^+ + C_2H_4$ observed when the reaction gas cell is filled with neutral C_2H_4 gas at a pressure of 0.1 mTorr. As expected, only the ion peaks at m/z = 28 and 29 are observed in the mass spectrum of Figure 1a, which are assigned to the N_2^+ and its isotopic form of $^{15}N^{14}N^+$, respectively. Four ion peaks are observed at m/z = 26, 27, 28, and 29, of which the first two can be assigned as $C_2H_2^+$ and $C_2H_3^+$ ions, respectively. For ions appearing at m/z = 28 of Figure 1b, we have assigned them as the unreacted N_2^+ ions. We note that one previous study[19] has reported the observation of $HCNH^+$ ions, which also have a m/z value of

DOI: 10.1021/acs.jpca.8b04587
J. Phys. Chem. A 2018, 122, 6491−6499

28. However, a most recent review work[22] suggested no $HCNH^+$ formation for this reaction system. It should be noted that our results alone cannot rule out the possible formation of $HCNH^+$ ions. Here, our mass spectrometric assignment follows the recommendation of the most recent review.[22]

Another possible ion observed at m/z = 28 in the spectrum of Figure 1b is the $C_2H_4^+$ ion, which could be produced by the charge-transfer collision. However, previous studies, including the unimolecular dissociation studies[43−45] of the $C_2H_4^+$ ion and the mass spectrometric study[21] of the $N_2^+ + C_2D_4$ isotopic reaction, strongly suggest that no stable $C_2H_4^+$ ions were formed in the $N_2^+ + C_2H_4$ reaction. Actually, the rationalization of rapid unimolecular dissociation[43−45] of excited $C_2H_4^+$ ions populated in a near-resonant charge-transfer collision of $N_2^+ + C_2H_4$ is consistent with the present experiment of finding $C_2H_3^+$ and $C_2H_2^+$ as the dominant product channels, which also supports that stable $C_2H_4^+$ product ions may not be formed.

For ions detected at m/z = 29, the possible ion structures are $N_2H^+/C_2H_5^+/{}^{15}N^{14}N^+$. Figure 2 depicts the time-of-flight (TOF) spectrum for m/z = 29 ions. The salient feature of this TOF spectrum is that it consists of a fast and sharp component and a slow and broad one. In addition, the peak intensity of the sharp component at the m/z = 29 position is higher than that when there is no C_2H_4 gas in the gas cell, which is verified by the reaction cross section measurements, indicating that new species with m/z of 29 are formed through reactions rather than $C_2H_5^+/{}^{15}N^{14}N^+$. On the basis of the energetic analysis and previous studies,[25] as well as our experimental observations, the fast and sharp component can be assigned as N_2H^+ product ions and the unreacted ${}^{15}N^{14}N^+$ ions. The TOF peak profile for N_2H^+ product ions formed via the H atom transfer stripping mechanism is observed to broaden only mildly compared to that of ${}^{15}N^{14}N^+$ reactant ions (as well as ${}^{14}N^{14}N^+$ reactant ions). Thus, the fast and sharp ion peak of Figure 2 can be assigned to $N_2H^+/{}^{15}N^{14}N^+$, whereas the broader TOF component of the m/z = 29 ions is assigned as $C_2H_5^+$ ions, which are formed by secondary reaction 4 between $C_2H_3^+$ product ions and neutral C_2H_4 molecules in the reaction gas cell. According to known energetic information, reaction 4 is exothermic with $\Delta E = -2.378$ eV, a value comparable to that from reactions 1−3.[42,46]

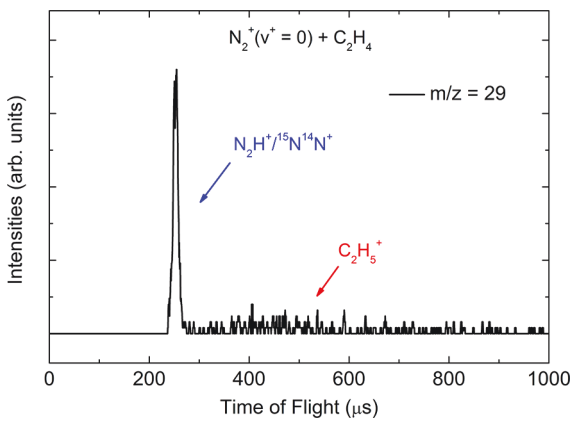

Figure 2. TOF spectrum of m/z = 29 ions. The fast and sharp TOF component is assigned as N_2H^+ and ${}^{15}N^{14}N^+$ ions, and the slow and broad TOF component is attributed to $C_2H_5^+$ ions produced by secondary reaction of $C_2H_3^+ + C_2H_4$, occurring in the reaction gas cell. E_{cm} is set at 0.30 eV for this measurement.

$$C_2H_3^+ + C_2H_4 \rightarrow C_2H_5^+ + C_2H_2 \qquad \Delta E = -2.378 \pm 0.006 \text{ eV} \tag{4}$$

The broad component of the TOF spectrum of Figure 2 is indicative that the secondary $C_2H_5^+$ ions have near-thermal kinetics energies. In a previous study of the $N_2^+ + CH_4$ reaction, identification of secondary $C_2H_5^+$ ions with near-thermal energies formed in the reaction gas cell has also been made by the TOF technique.[8]

In the present experiment, if the secondary reaction between $C_2H_3^+$ and C_2H_4 occurs, it seems straightforward to anticipate that another secondary reaction between $C_2H_2^+$ and C_2H_4 could also take place. On the basis of one of the previous studies,[20] three product ions, $C_2H_4^+$, $C_3H_3^+$, and $C_4H_5^+$, with a corresponding BR of 0.30:0.48:0.22, are expected to be formed by the $C_2H_2^+ + C_2H_4$ reaction. However, because we did not observe any product ions at m/z = 39 and 53 in the mass spectrometric measurements, such as that shown in Figure 1b, we have assumed that occurrence of the latter secondary reaction of $C_2H_2^+ + C_2H_4$ is negligible. We note that the assignments of the mass spectra of Figures 1b and 2 are consistent with the recommendations given in the most recent review[22] on the title ion−molecule reaction system.

The contribution of ${}^{15}N^{14}N^+$ ions to the observed intensity of the m/z = 29 ion peak can be corrected by taking the difference of the m/z = 29 ion peak intensities observed with and without reactant C_2H_4 gas filled in the reaction gas cell. After subtracting out the ${}^{15}N^{14}N^+$ ion contribution, the remaining m/z = 29 ions can be ascribed to the sum of the N_2H^+ and $C_2H_5^+$ ions, where the $C_2H_5^+$ ions can be determined by gating the ion counts measured within the slow and broad TOF components shown in Figure 2. Measurement of these $C_2H_5^+$ ions allows determination of the actual intensities for product N_2H^+ ions. On the basis of the interpretation and thus assignment of the mass spectra, we attributed the observed $C_2H_5^+$ ion signal as part of that for the product $C_2H_3^+$ ion. The contributions from $C_2H_5^+$ ions to the final $\sigma_{\nu+}(C_2H_3^+)$ values shown in Figure 3a (which are discussed below) are about in the range of 15 ± 5% in the E_{cm} range reported in this work.

Kinetic Energy Dependence. The $\sigma_{\nu+}(C_2H_3^+)$, $\sigma_{\nu+}(C_2H_2^+)$, and $\sigma_{\nu+}(N_2H^+)$, ν^+ = 0−2, curves determined in the E_{cm} range of 0.05−10.00 eV based on intensity measurements for the three primary product ions $C_2H_3^+$, $C_2H_2^+$, and N_2H^+ are depicted in Figure 3a−c, respectively. Their σ values are in the order of $\sigma_{\nu+}(C_2H_3^+) > \sigma_{\nu+}(C_2H_2^+) > \sigma_{\nu+}(N_2H^+)$. As shown in Figure 3a,b, the trends and profiles of the $\sigma_{\nu+}(C_2H_3^+)$ and $\sigma_{\nu+}(C_2H_2^+)$ curves are very similar. As E_{cm} is increased, a slow decrease is observed for both $\sigma_{\nu+}(C_2H_3^+)$ and $\sigma_{\nu+}(C_2H_2^+)$ at $E_{cm} \leq 0.10$ eV. In the E_{cm} range of 0.20−3.00 eV, both the $\sigma_{\nu+}(C_2H_3^+)$ and the $\sigma_{\nu+}(C_2H_2^+)$ become nearly constant. The $\sigma_{\nu+=2}$ $(C_2H_3^+)$ $[\sigma_{\nu+=2}(C_2H_2^+)]$ is found to decrease rapidly from about 110 Å^2 [70 Å^2] at E_{cm} = 3.00 eV to about 10 Å^2 at E_{cm} = 10.00 eV. As shown in Figure 3c, the minor $\sigma_{\nu+}(N_2H^+)$ appears to decrease exponentially as E_{cm} is increased, from about 10 Å^2 at E_{cm} = 0.05 eV to vanishingly low values (<0.05 Å^2) at E_{cm} > 0.7 eV.

The sum of the integral cross sections for all of the product channels, i.e., $\sigma_{\nu+}(\text{sum}) = \sigma_{\nu+}(C_2H_3^+) + \sigma_{\nu+}(C_2H_2^+) + \sigma_{\nu+}(N_2H^+)$, is a measure of the overall chemical reactivity of $N_2^+(X^2\Sigma_g^+; \nu^+)$ toward C_2H_4. We obtained the $\sigma_{\nu+}(\text{sum})$, ν^+ =

DOI: 10.1021/acs.jpca.8b04587
J. Phys. Chem. A 2018, 122, 6491−6499

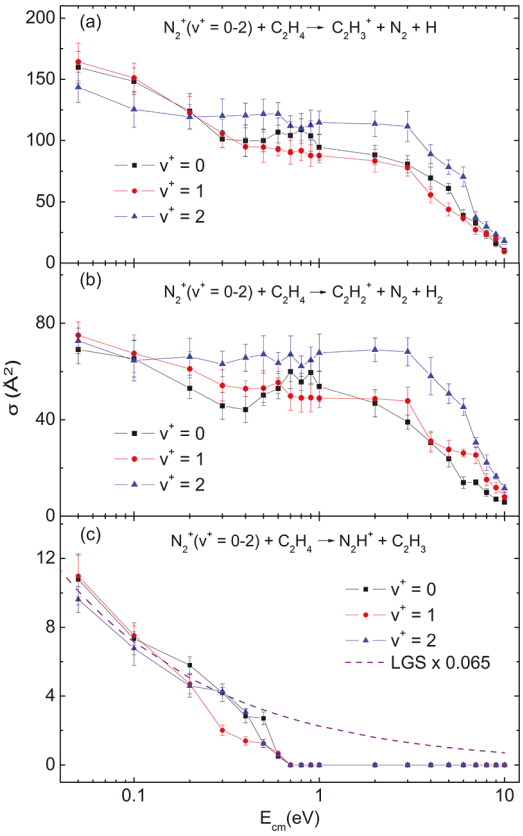

Figure 3. Absolute integral cross sections for (a) $C_2H_3^+$, (b) $C_2H_2^+$, and (c) N_2H^+ reaction channels, plotted as a function of E_{cm} and ν^+ vibrational excitation of N_2^+ ions. The $\sigma_{\nu+}$ values for $\nu^+ = 0$, 1, and 2 are shown as black square, red dot, and green triangle curves, respectively. For comparison, a scaled LGS curve[47] by a factor of 0.065 is also shown in (c) with a dashed purple line. In addition, $\sigma_{\nu+} = 0$ when $E_{cm} > 0.7$ eV in (c) means that the experimental values are below 0.05 Å^2.

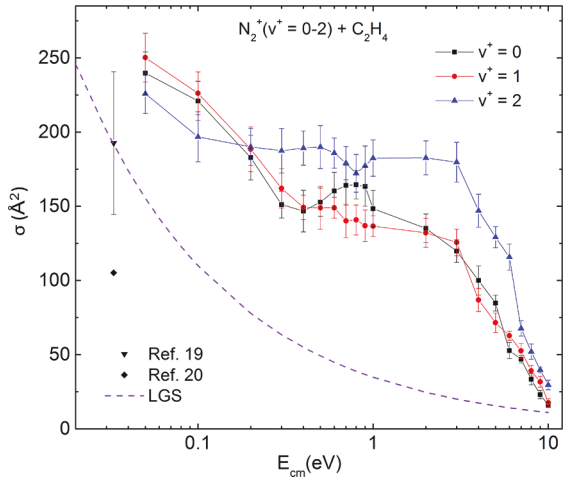

Figure 4. Comparison of the $\sigma_{\nu+}$(sum) obtained here with σ values converted from k_r values obtained in previous kinetics measurements[19,20] as well as σ(LGS) predictions.[47] The $\sigma_{\nu+}$(sum) curves for the $\nu^+ = 0$, 1, and 2 vibrational states of N_2^+ ions are shown as the black square, red dot, and blue triangle curves, respectively. The theoretical σ(LGS) predictions are depicted with the dashed purple line in the figure.

0−2, curves as shown in Figure 4 to compare with the results of previous kinetics measurements as well as the σ predictions [σ(LGS)'s] based on the Langevin−Gioumousis−Stevenson (LGS) capture model.[47] Due to the significantly smaller value of $\sigma_{\nu+}(N_2H^+)$ than those of $\sigma_{\nu+}(C_2H_3^+)$ and $\sigma_{\nu+}(C_2H_2^+)$, the profile for $\sigma_{\nu+}$(sum) is similar to those for $\sigma_{\nu+}(C_2H_3^+)$ and $\sigma_{\nu+}(C_2H_2^+)$. In the present study, the k_r values obtained from previous chemical kinetic studies are converted to σ values using the approximated formula $k_r = \sigma\langle v\rangle$, where $\langle v\rangle$ is the average velocity of the colliding pair, which can be calculated for a given E_{cm}. Because the reaction temperatures were not mentioned in the previous k_r measurements, we assume that the temperature involved is room temperature (300 K) for all kinetics work cited here. According to the LGS model, the integral cross section can be calculated using the formula $\sigma(\text{LGS}) = (2\pi e/\langle v\rangle) \times (\alpha/\mu)$, where e is the electron charge, α stands for the polarizability (4.252×10^{-24} cm^3) of the C_2H_4 molecule,[48] and μ is the reduced mass for the colliding pair. Thus, the LGS model predicts that the σ(LGS) falls as a function of $(E_{cm})^{-1/2}$.

The $\sigma_{\nu+}$(sum) values obtained here (shown in Figure 4) are significantly higher than the σ values converted from previous kinetics measurements as well as the σ(LGS) predictions. Such discrepancy indicates that the LGS model may be over-simplified for the $N_2^+ + C_2H_4$ reaction system. The LGS model only treats the ion−molecule interaction as one between a charge and an induced dipole (without taking into account any internal quantum level structures). The much larger $\sigma_{\nu+}$(sum) compared to the σ(LGS) observed here suggests that a different reaction mechanism, which may include a long-range electron jump process, results in high chemical reactivity.

As pointed out above, the trends and profiles of the $\sigma_{\nu+}(C_2H_3^+)$, $\sigma_{\nu+}(C_2H_2^+)$, and $\sigma_{\nu+}$(sum) curves obtained here are very similar, but they are quite different from that of the σ(LGS), which is predicted to fall as a function of $(E_{cm})^{-1/2}$. This observation also indicates that the mechanism for the $N_2^+ + C_2H_4$ reaction is quite different from that predicted based on the LGS model. The similar profiles observed for the $\sigma_{\nu+}(C_2H_3^+)$ and $\sigma_{\nu+}(C_2H_2^+)$ strongly suggest that the $C_2H_3^+$ and $C_2H_2^+$ product channels are governed by a similar reaction mechanism. Observation of high $\sigma_{\nu+}(C_2H_3^+)$ and $\sigma_{\nu+}(C_2H_2^+)$ values suggests that the collision-assisted dissociative charge-transfer mechanism is operative in the formation of $C_2H_3^+$ and $C_2H_2^+$ product ions. This mechanism has also been suggested to be operative in the ion−molecule reactions of $N_2^+(X^2\Sigma_g^+: \nu^+ = 0\text{−}2) + CH_4$ (C_2H_2 and H_2O).[8,9] For the present reaction, the dissociative charge-transfer reaction mechanism would first involve the production of internally excited $C_2H_4^{+*}$ intermediates by energy-resonance or near-energy-resonance charge-transfer collisions of $N_2^+(X^2\Sigma_g^+; \nu^+) + C_2H_4$. This is to be followed by the rapid unimolecular dissociation of $C_2H_4^{+*}$ into the $C_2H_3^+ + H$ and $C_2H_2^+ + H_2$ product states.

To assist the discussion below, we show in Figure 5 the potential energy diagram for the $N_2^+(X^2\Sigma_g^+: \nu^+ = 0\text{−}2) + C_2H_4(X)$ reaction system in the heat of formation scale. Here, the reactant states $N_2^+(X: \nu^+ = 0\text{−}2) + C_2H_4(X)$ (shown in black), along with the observed product states, $C_2H_3^+(X) + N_2(X) + H$, $C_2H_2^+(X) + N_2(X) + H_2(X)$, and $N_2H^+(X) + C_2H_3(X)$ (shown in red), and the unobserved product state $C_2H_4^+(X) + N_2(X)$ (shown in blue) are shown in the figure. On the left-hand side of Figure 5, we post a vibrationally resolved HeI photoelectron spectrum covering the formation of vibronic bands of the $C_2H_4^+$(X, A, B, and C) states.[49] As

DOI: 10.1021/acs.jpca.8b04587
J. Phys. Chem. A 2018, 122, 6491−6499

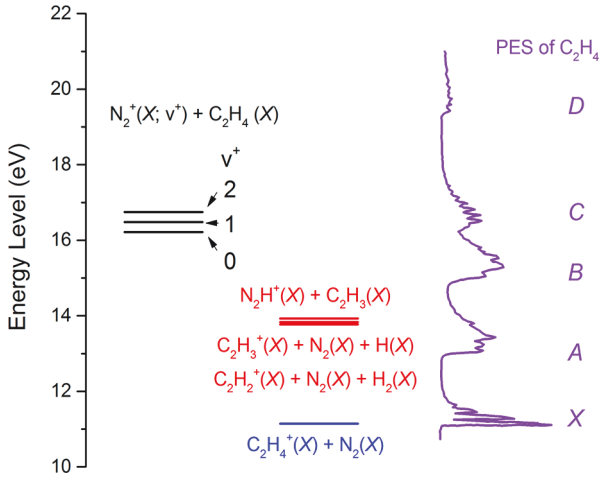

Figure 5. Potential energy diagram for the $N_2^+(X^2\Sigma_g^+: \nu^+ = 0-2)$ + $C_2H_4(X)$ reaction system in the heat of formation scale. Here, the reactant states $N_2^+(X: \nu^+ = 0-2)$ + $C_2H_4(X)$ (shown in black), along with the observed product states, $C_2H_3^+(X)$ + $N_2(X)$ + H, $C_2H_2^+(X)$ + $N_2(X)$ + $H_2(X)$, and $N_2H^+(X)$ + $C_2H_3(X)$ (shown in red), and the unobserved product state $C_2H_4^+(X)$ + $N_2(X)$ (shown in blue) are shown in the figure. On the left-hand side, a vibrationally resolved HeI photoelectron spectrum[49] covering the formation of vibronic bands of the $C_2H_4^+$(X, A, B, and C) states is shown in purple.

shown in the figure, the $N_2^+(X: \nu^+ = 0-2)$ + $C_2H_4(X)$ reactant states are in energy-resonance with the $C_2H_4^+(C)$ + N_2 states, which is more than 2 eV above the onsets for the production of $C_2H_3^+(X)$ + N_2 + H and $C_2H_2^+(X)$ + N_2 + H_2 product states. Thus, the formation of $C_2H_3^+(X)$ and $C_2H_2^+(X)$ product ions from the unimolecular dissociation of excited $C_2H_4^{+*}$ intermediates is expected to be prompt.[43−45] On the basis of the potential energy diagram, the excitation to both $C_2H_4^+$(B, C) states is strongly dissociative. The previous quantum-state or energy-selected unimolecular dissociation measurements[50,51] of the breakdown curves for the formation of $C_2H_2^+$ and $C_2H_3^+$ ions from $C_2H_4^+$ also support this conclusion. We note that the $C_2H_4^+$(B, C) states involved in this discussion also include rovibrational excitations. The near-energy-resonance $C_2H_4^+$(B) state can be populated by collision-induced or E_{cm}-assisted processes. Without a detailed theoretical interpretation for this reaction system, we have attributed the high $\sigma_{\nu+}(C_2H_3^+)$ and $\sigma_{\nu+}(C_2H_2^+)$ values observed to E_{cm}-assisted nonadiabatic interactions between the $N_2^+(X: \nu^+ = 0-2)$ + C_2H_4 reactant states and near-energy-resonance $C_2H_4^+$(B, C) + N_2 states. The E_{cm}-assisted nonadiabatic coupling is expected to enhance the interaction between the reactant states and the $C_2H_4^+$(B, C) + N_2 intermediate states with finite energy mismatches and thus results in the formation of $C_2H_4^{+*}$ intermediates [or $C_2H_4^+$(B, C)] with higher intensities. Because charge-transfer $C_2H_4^{+*}$ intermediates thus formed would undergo rapid dissociation, the production of more intense $C_2H_4^{+*}$ intermediates would translate into higher $C_2H_3^+$ and $C_2H_2^+$ ion intensities. This nonadiabatic pathway can compensate the decrease of the $\sigma_{\nu+}$ due to the increase of E_{cm} in the LGS model. However, the trend of maintaining high $\sigma_{\nu+}(C_2H_3^+)$ and $\sigma_{\nu+}(C_2H_2^+)$ seems to end at $E_{cm} \geq 3.00$ eV.

The trends and profiles of the $\sigma_{\nu+}(C_2H_3^+)$ and $\sigma_{\nu+}(C_2H_2^+)$ curves are different from those of the $\sigma_{\nu+}(N_2H^+)$ curve, which exhibits an exponential decreasing trend as E_{cm} is increased from thermal energy. For the formation of the N_2H^+ product ions, a reaction path of H atom transfer is needed that requires short-range collisions between the N_2^+ ion and C_2H_4 molecule. Therefore, the reaction mechanism for forming the N_2H^+ product ions is different from that for $C_2H_2^+$ and $C_2H_3^+$ ions discussed above. The $\sigma_{\nu+}(N_2H^+)$ is the minor product channel, which represents ≤5% of the total product ion intensity. The N_2H^+ ion signal is found to nearly disappear at $E_{cm} \geq 0.70$ eV

Table 1. BRs of the $C_2H_3^+$, $C_2H_2^+$, and N_2H^+ Reaction Channels of the Quantum-Vibrational-State-Selected Ion−Molecule Reaction of $N_2^+(X^2\Sigma_g^+; \nu^+ = 0-2)$ + C_2H_4 Measured in the E_{cm} Range from 0.05 to 10.00 eV[a]

	$\nu^+ = 0$			$\nu^+ = 1$			$\nu^+ = 2$		
E_{cm}(eV)	$C_2H_3^+$	$C_2H_2^+$	N_2H^+	$C_2H_3^+$	$C_2H_2^+$	N_2H^+	$C_2H_3^+$	$C_2H_2^+$	N_2H^+
0.05	0.65 ± 0.05	0.30 ± 0.04	0.05 ± 0.01	0.66 ± 0.04	0.29 ± 0.04	0.05 ± 0.01	0.64 ± 0.05	0.32 ± 0.04	0.04 ± 0.01
0.10	0.65 ± 0.05	0.31 ± 0.04	0.04 ± 0.01	0.68 ± 0.04	0.28 ± 0.04	0.04 ± 0.01	0.65 ± 0.05	0.32 ± 0.04	0.03 ± 0.01
0.20	0.66 ± 0.04	0.31 ± 0.04	0.03 ± 0.01	0.65 ± 0.05	0.31 ± 0.04	0.04 ± 0.01	0.64 ± 0.05	0.34 ± 0.04	0.02 ± 0.01
0.30	0.65 ± 0.05	0.32 ± 0.05	0.03 ± 0.01	0.65 ± 0.05	0.32 ± 0.04	0.03 ± 0.01	0.64 ± 0.05	0.33 ± 0.04	0.03 ± 0.01
0.40	0.65 ± 0.05	0.33 ± 0.05	0.02 ± 0.01	0.64 ± 0.05	0.34 ± 0.04	0.02 ± 0.01	0.64 ± 0.05	0.34 ± 0.04	0.02 ± 0.01
0.50	0.62 ± 0.05	0.36 ± 0.05	0.02 ± 0.01	0.63 ± 0.05	0.34 ± 0.04	0.02 ± 0.01	0.65 ± 0.05	0.34 ± 0.04	0.01 ± <0.01
0.60	0.62 ± 0.05	0.37 ± 0.05	0.01 ± <0.01	0.62 ± 0.05	0.36 ± 0.05	0.02 ± 0.01	0.66 ± 0.04	0.33 ± 0.04	0.01 ± <0.01
0.70	0.58 ± 0.05	0.42 ± 0.05	<0.01	0.64 ± 0.05	0.36 ± 0.05	<0.01	0.63 ± 0.05	0.37 ± 0.05	<0.01
0.80	0.62 ± 0.05	0.38 ± 0.05	<0.01	0.64 ± 0.05	0.36 ± 0.05	<0.01	0.64 ± 0.05	0.36 ± 0.05	<0.01
0.90	0.58 ± 0.05	0.42 ± 0.05	<0.01	0.64 ± 0.05	0.36 ± 0.05	<0.01	0.64 ± 0.05	0.36 ± 0.05	<0.01
1.00	0.58 ± 0.05	0.42 ± 0.05	<0.01	0.63 ± 0.05	0.37 ± 0.05	<0.01	0.63 ± 0.05	0.37 ± 0.05	<0.01
2.00	0.61 ± 0.05	0.39 ± 0.05	<0.01	0.61 ± 0.05	0.39 ± 0.05	<0.01	0.63 ± 0.05	0.37 ± 0.05	<0.01
3.00	0.63 ± 0.05	0.37 ± 0.05	<0.01	0.61 ± 0.05	0.39 ± 0.05	<0.01	0.63 ± 0.05	0.37 ± 0.05	<0.01
4.00	0.67 ± 0.04	0.33 ± 0.04	<0.01	0.63 ± 0.05	0.37 ± 0.05	<0.01	0.61 ± 0.05	0.39 ± 0.05	<0.01
5.00	0.71 ± 0.04	0.29 ± 0.04	<0.01	0.60 ± 0.05	0.40 ± 0.05	<0.01	0.61 ± 0.05	0.39 ± 0.05	<0.01
6.00	0.72 ± 0.04	0.28 ± 0.04	<0.01	0.57 ± 0.05	0.43 ± 0.05	<0.01	0.61 ± 0.05	0.39 ± 0.05	<0.01
7.00	0.68 ± 0.04	0.32 ± 0.04	<0.01	0.50 ± 0.05	0.50 ± 0.05	<0.01	0.55 ± 0.05	0.45 ± 0.05	<0.01
8.00	0.69 ± 0.04	0.31 ± 0.04	<0.01	0.58 ± 0.05	0.42 ± 0.05	<0.01	0.58 ± 0.05	0.42 ± 0.05	<0.01
9.00	0.67 ± 0.04	0.33 ± 0.04	<0.01	0.59 ± 0.05	0.41 ± 0.05	<0.01	0.60 ± 0.05	0.40 ± 0.05	<0.01
10.00	0.58 ± 0.05	0.42 ± 0.05	<0.01	0.52 ± 0.05	0.48 ± 0.05	<0.01	0.61 ± 0.05	0.39 ± 0.05	<0.01

[a]The standard deviations are estimated based on the reproducibility of independent measurements.

DOI: 10.1021/acs.jpca.8b04587
J. Phys. Chem. A 2018, 122, 6491−6499

($\sigma_{\nu+}(N_2H^+)$ < 0.05 Å^2). We note that the almost exponential deceasing trend of $\sigma_{\nu+}(N_2H^+)$ observed as a function of E_{cm} does not agree with the prediction from the classical LGS model,[47] which predicts σ to be proportional to $(E_{cm})^{-1/2}$. For comparison, a scaled LGS curve by a factor of 0.065 is shown in Figure 3c with a dashed purple line. Below E_{cm} = 0.3 eV, the scaled LGS curve fits well with our experimental values. However, deviations start to be observed when E_{cm} > 0.3 eV. Therefore, rigorous theoretical chemical dynamics calculations are called for in order to better understand the detailed E_{cm} effects observed here.

Vibrational-State Dependence. The ν^+-vibrational effect for the title reaction can be observed in the comparison of the ν^+ = 0−2 curves for $\sigma_{\nu+}(C_2H_3^+)$, $\sigma_{\nu+}(C_2H_2^+)$, and $\sigma_{\nu+}(N_2H^+)$, as shown in Figure 3a−c, respectively. No vibrational effect is observed for the minor $\sigma_{\nu+}(N_2H^+)$ channel. The comparison of the ν^+ = 0−2 curves reveals very similar ν^+-vibrational effects for $\sigma_{\nu+}(C_2H_3^+)$ and $\sigma_{\nu+}(C_2H_2^+)$, which again indicates that these product channels are formed through similar reaction mechanisms. For the $\sigma_{\nu+}(C_2H_3^+)$ and $\sigma_{\nu+}(C_2H_2^+)$ reaction channels, excitations to the ν^+ = 0 and 1 vibrational states of the N_2^+ reactant ions yield very similar $\sigma_{\nu+}$ curves. Excitation to the ν^+ = 2 state shows clearly the enhancement effect at 0.20 < E_{cm} < 7.00 eV. At 0.20 < E_{cm} ≤ 1.00 eV, the $\sigma_{\nu+}(C_2H_3^+)$ and $\sigma_{\nu+}(C_2H_2^+)$ values for ν^+ = 2 are about 15% higher than those for ν^+ = 0 and 1, while at 1.00 < E_{cm} < 7.00 eV, the enhancements for ν^+ = 2 are found to increase to 30−40%. Such vibrational enhancement on reactivity for the ν^+ = 2 state may be rationalized by a long-range "near-resonance" dissociative charge-transfer reaction mechanism. As shown in Figure 5, the energetic level of the $N_2^+ + C_2H_4$ with N_2^+ at ν^+ = 2 state is more "resonant" with the peak positions of the $C_2H_4^+$(C) state, compared to that of N_2^+ at ν^+ = 0 or 1 states. The fact that $\sigma_{\nu+}(N_2H^+)$ has different vibrational effects from that of $\sigma_{\nu+}(C_2H_3^+)$ and $\sigma_{\nu+}(C_2H_2^+)$ also suggests that different reaction mechanisms are involved for these reaction channels. The vibrational effects observed for the $\sigma_{\nu+}$(sum), ν^+ = 0−2, curves shown in Figure 4 are similar to those for the $\sigma_{\nu+}(C_2H_3^+)$ and $\sigma_{\nu+}(C_2H_2^+)$, ν^+ = 0−2, curves plotted in Figure 3a,b. As pointed out above, this observation is due to the fact that $C_2H_3^+$ and $C_2H_2^+$ ions are the dominant product ions in the E_{cm} range of interest. Better understanding of the complex ν^+-vibrational effects observed in Figures 3a−c and 4 would require a rigorous theoretical investigation. In addition, similar to our previous works of N_2^+(X) + Ar,[29] N_2^+(X) + CH_4,[8] N_2^+(X) + C_2H_2,[9] and N_2^+(X) + H_2O,[10] no rotational dependence has been observed for the present reaction system.

Branching Ratios. Table 1 lists detailed BRs for the three reaction channels determined as a function of both ν^+-vibrational excitations of N_2^+ and E_{cm} covering the E_{cm} range from 0.05 to 10.00 eV. These BRs were obtained by comparing the relative intensities of the $C_2H_3^+$, $C_2H_2^+$, and N_2H^+ product ions measured at selected E_{cm} values, and thus, the uncertainty can achieve a value of ±5%. At E_{cm} ≤ 0.60 eV, the BRs for all three vibrational states (ν^+ = 0−2) are nearly identical at the same E_{cm}. At E_{cm} = 0.05 eV, which corresponds to a reaction temperature of ∼580 K, the BR of $C_2H_3^+$:$C_2H_2^+$:N_2H^+ is determined here to be 65%:30%:5%, which is close to the recommended value[22] of 0.67%:0.23%:10% determined at a reaction temperature of 300 K. As E_{cm} is increased from 0.05 to 0.70 eV, the branching fraction of the N_2H^+ ion gradually decreases from 5% to 0, the branching fraction of the $C_2H_2^+$ ion increases from 30 to 35%, and the branching fraction of the $C_2H_3^+$ ion remains at about 65%. At 0.70 ≤ E_{cm} ≤ 10.00 eV, the BR of $C_2H_3^+$:$C_2H_2^+$ is found to be almost constant with a value of (60 ± 5%):(40 ± 5%).

4. SUMMARY AND CONCLUSIONS

The quantum-vibrational-state-selected ion−molecule reaction $N_2^+(X^2\Sigma_g^+$: ν^+ = 0−2) + C_2H_4 has been investigated by employing a novel VUV-PFI-PI ion source together with a DQDO mass filter developed in our laboratory. Three product channels leading to the formation of $C_2H_3^+$, $C_2H_2^+$, and N_2H^+ ions are identified. This experiment has allowed detailed measurements for the $\sigma_{\nu+}(C_2H_3^+)$, $\sigma_{\nu+}(C_2H_2^+)$, and $\sigma_{\nu+}(N_2H^+)$, ν^+ = 0−2, and product BR ($C_2H_2^+$:$C_2H_3^+$:N_2H^+) values in the E_{cm} range from 0.05 to 10.00 eV. The $\sigma_{\nu+}(C_2H_3^+)$ and $\sigma_{\nu+}(C_2H_2^+)$ curves are found to be very similar, indicating that they are governed by a similar reaction mechanism. On the basis of this observation, we suggest that both $C_2H_3^+$ and $C_2H_2^+$ ions are formed by the collision-assisted dissociative charge-transfer mechanism. The $\sigma_{\nu+}(N_2H^+)$ curve obtained here has a different profile compared to those of the $\sigma_{\nu+}(C_2H_3^+)$ and $\sigma_{\nu+}(C_2H_2^+)$ curves, indicating that the formation of N_2H^+ is governed by the direct H atom transfer mechanism. Complex E_{cm} and vibrational dependences are observed for $\sigma_{\nu+}(C_2H_3^+)$ and $\sigma_{\nu+}(C_2H_2^+)$, ν^+ = 0−2. Clear vibrational enhancements are observed for the $\sigma_{\nu+}(C_2H_3^+)$ and $\sigma_{\nu+}(C_2H_2^+)$ channels with excitation to the ν^+ = 2 state. The $\sigma_{\nu+}$ and BR measurements obtained in the present work are valuable contributions to the database that can be used for modeling of the chemical compositions and their evolutions of Titan's atmosphere and for benchmarking state-of-the-art theoretical calculations on the chemical reaction dynamics of the title reaction system.

■ AUTHOR INFORMATION

Corresponding Author

*E-mail: cyng@ucdavis.edu.

ORCID

Yuntao Xu: 0000-0002-1205-8168

Cheuk-Yiu Ng: 0000-0003-4425-5307

Notes

The authors declare no competing financial interest.

■ ACKNOWLEDGMENTS

This material is based upon work supported by the National Science Foundation under CHE-1763319. C.Y.N. is also grateful to Dr. Huie Tarng Liou for his generous donation of research support for the Ng Laboratory. The authors are also grateful to the reviewers for their careful reading and detailed comments of the manuscript.

■ REFERENCES

(1) Bohme, D. K. PAH [Polycyclic Aromatic Hydrocarbons] and Fullerene Ions and Ion/Molecule Reactions in Interstellar and Circumstellar Chemistry. *Chem. Rev.* **1992**, *92* (7), 1487−1508.

(2) Snow, T. P.; Bierbaum, V. M. Ion Chemistry in the Interstellar Medium. *Annual Review of Analytical Chemistry*; Annual Reviews: Palo Alto, CA, 2008; Vol. *1*, pp 229−259.

(3) Giguere, P. T.; Huebner, W. F. A Model of Comet Comae. I. Gas-Phase Chemistry in One Dimension. *Astrophys. J.* **1978**, *223*, 638.

(4) Huntress, W. T., Jr; McEwan, M. J.; Karpas, Z.; Anicich, V. G. Laboratory Studies of Some of The Major Ion−Molecule Reactions Occurring in Cometary Comae. *Astrophys. J., Suppl. Ser.* **1980**, *44*, 481.

DOI: 10.1021/acs.jpca.8b04587
J. Phys. Chem. A 2018, 122, 6491−6499

(5) Smith, D.; Spanel, P. Ions in the Terrestrial Atmosphere and in Interstellar Clouds. *Mass Spectrom. Rev.* **1995**, *14* (4−5), 255−278.
(6) Williams, K. L.; Martin, I. T.; Fisher, E. R. On the Importance of Ions and Ion−Molecule Reactions to Plasma-Surface Interface Reactions. *J. Am. Soc. Mass Spectrom.* **2002**, *13* (5), 518−529.
(7) Semo, N. M.; Koski, W. S. Some Ion−Molecule Reactions Pertinent to Combustion. *J. Phys. Chem.* **1984**, *88* (22), 5320−5324.
(8) Xu, Y.; Chang, Y. C.; Lu, Z.; Ng, C. Y. Absolute Integral Cross Sections and Product Branching Ratios for the Vibrationally Selected Ion−Molecule Reactions: $N_2^+(X^2\Sigma_g^+; v^+ = 0-2) + CH_4$. *Astrophys. J.* **2013**, *769* (1), 72.
(9) Xu, Y.; Xiong, B.; Chang, Y. C.; Ng, C. Y. Absolute Integral Cross Sections for the State-selected Ion−Molecule Reaction $N_2^+(X^2\Sigma_g^+; v^+ = 0-2) + C_2H_2$ in the Collision Energy Range of 0.03−10.00 eV. *Astrophysical Journal* **2016**, *827* (1), 17.
(10) Xu, Y.; Xiong, B.; Chang, Y. C.; Ng, C.-Y. Quantum-Vibrational-State-Selected Integral Cross Sections and Product Branching Ratios for the Ion−Molecule Reactions of $N_2^+(X^2\Sigma_g^+; v^+ = 0-2) + H_2O$ and $H_2O^+(X^2B_1: v_1^+v_2^+v_3^+ = 000$ and $100) + N_2$ in the Collision Energy Range of 0.04−10.00 eV. *Astrophysical Journal* **2018**, *861* (1), 17.
(11) Colwell, J. Titan: the Planet Moon. *The Ringed Planet*; Morgan & Claypool Publishers, 2017; pp 6-1−6-16.
(12) Kuiper, G. P. Titan: a Satellite with an Atmosphere. *Astrophys. J.* **1944**, *100*, 378.
(13) Lindal, G. F.; Wood, G. E.; Hotz, H. B.; Sweetnam, D. N.; Eshleman, V. R.; Tyler, G. L. The Atmosphere of Titan: An Analysis of the Voyager 1 Radio Occultation Measurements. *Icarus* **1983**, *53* (2), 348−363.
(14) Niemann, H. B.; Atreya, S. K.; Bauer, S. J.; Carignan, G. R.; Demick, J. E.; Frost, R. L.; Gautier, D.; Haberman, J. A.; Harpold, D. N.; Hunten, D. M.; et al. The Abundances of Constituents of Titan's Atmosphere from the GCMS Instrument on the Huygens Probe. *Nature* **2005**, *438* (7069), 779−784.
(15) Shemansky, D. E.; Stewart, A. I. F.; West, R. A.; Esposito, L. W.; Hallett, J. T.; Liu, X. The Cassini UVIS Stellar Probe of the Titan Atmosphere. *Science* **2005**, *308* (5724), 978−982.
(16) Schinder, P. J.; Flasar, F. M.; Marouf, E. A.; French, R. G.; McGhee, C. A.; Kliore, A. J.; Rappaport, N. J.; Barbinis, E.; Fleischman, D.; Anabtawi, A. The Structure of Titan's Atmosphere from Cassini Radio Occultations. *Icarus* **2011**, *215* (2), 460−474.
(17) Anicich, V. G.; McEwan, M. J. Ion−Molecule Chemistry in Titan's Ionosphere. *Planet. Space Sci.* **1997**, *45* (8), 897−921.
(18) Lebreton, J.-P.; Witasse, O.; Sollazzo, C.; Blancquaert, T.; Couzin, P.; Schipper, A.-M.; Jones, J. B.; Matson, D. L.; Gurvits, L. I.; Atkinson, D. H.; et al. An Overview of the Descent and Landing of the Huygens Probe on Titan. *Nature* **2005**, *438* (7069), 758−764.
(19) McEwan, M. J.; Scott, G. B. I.; Anicich, V. G. Ion−Molecule Reactions relevant to Titan's Ionosphere. *Int. J. Mass Spectrom. Ion Processes* **1998**, *172* (3), 209−219.
(20) Anicich, V. G.; Wilson, P.; McEwan, M. J. A SIFT Ion−Molecule Study of Some Reactions in Titan's Atmosphere. Reactions of N^+, N_2^+, and HCN^+ with CH_4, C_2H_2, and C_2H_4. *J. Am. Soc. Mass Spectrom.* **2004**, *15* (8), 1148−1155.
(21) Gichuhi, W. K.; Suits, A. G. Primary Branching Ratios for the Low-Temperature Reaction of State-Prepared N_2^+ with CH_4, C_2H_2, and C_2H_4. *J. Phys. Chem. A* **2011**, *115* (25), 7105−7111.
(22) Dutuit, O.; Carrasco, N.; Thissen, R.; Vuitton, V.; Alcaraz, C.; Pernot, P.; Balucani, N.; Casavecchia, P.; Canosa, A.; Le Picard, S.; et al. Critical Review of N,N^+, N_2^+, N^{+2}, and N_2^{+2} Main Production Processes and Reactions of Relevance to Titan's Atmosphere. *Astrophys. J., Suppl. Ser.* **2013**, *204* (2), 20.
(23) Anderson, S. L. Multiphoton Ionization State Selection: Vibrational-Mode and Rotational-State Control. In *Advances in Chemical Physics: State-Selected and State-To-State Ion−Molecule Reaction Dynamics, Part 1. Experiment*; Ng, C.-Y., Baer, M., Eds.; John Wiley & Sons, Inc., 1992; Vol. *82*, pp 177−212.
(24) Koyano, I.; Tanaka, K. State Selected Charge Transfer and Chemical Reactions by the TESICO Technique. In *Advances in Chemical Physics, Vol. 82, Part 1: State Selected and State to State Ion Molecule Reaction Dynamics: Experiment*; Ng, C.-Y., Baer, M., Eds.; John Wiley & Sons, Inc., 1992; Vol. *82*, pp 263−308.
(25) Ng, C.-Y. State-Selected and State-to-State Ion-Molecular Reaction Dynamics by Photoionization and Differential Reactivity Methods. In *Advances in Chemical Physics: State-Selected and State-To-State Ion−Molecule Reaction Dynamics, Part 1. Experiment*; Ng, C.-Y., Baer, M., Eds.; John Wiley & Sons, Inc., 1992; Vol. *82*, pp 401−500.
(26) Ng, C.-Y. State-Selected and State-to-State Ion−Molecule Reaction Dynamics. *J. Phys. Chem. A* **2002**, *106* (25), 5953−5966.
(27) Dressler, R. A.; Chiu, Y.; Levandier, D. J.; Tang, X. N.; Hou, Y.; Chang, C.; Houchins, C.; Xu, H.; Ng, C.-Y. The Study of State-Selected Ion−Molecule Reactions Using the Vacuum Ultraviolet Pulsed Field Ionization-Photoion Technique. *J. Chem. Phys.* **2006**, *125* (13), 132306−14.
(28) Chang, Y. C.; Xu, H.; Xu, Y.; Lu, Z.; Chiu, Y.-H.; Levandier, D. J.; Ng, C. Y. Communication: Rovibrationally Selected Study of the $N_2^+(X; v^+ = 1, N^+ = 0-8)$ + Ar Charge Transfer Reaction Using the Vacuum Ultraviolet Laser Pulsed Field Ionization-Photoion Method. *J. Chem. Phys.* **2011**, *134* (20), 201105.
(29) Chang, Y. C.; Xu, Y.; Lu, Z.; Xu, H.; Ng, C. Y. Rovibrationally Selected Ion−Molecule Collision Study Using the Molecular Beam Vacuum Ultraviolet Laser Pulsed Field Ionization-Photoion Method: Charge Transfer Reaction of $N_2^+(X^2\Sigma_g^+; v^+ = 0-2; N^+ = 0-9)$ + Ar. *J. Chem. Phys.* **2012**, *137* (10), 104202.
(30) Xu, Y.; Xiong, B.; Chang, Y. C.; Ng, C. Y. Communication: Rovibrationally Selected Absolute Total Cross Sections for the Reaction $H_2O^+(X^2B_1: v_1^+v_2^+v_3^+ = 000; N^+Ka+Kc+) + D_2$: Observation of the Rotational Enhancement Effect. *J. Chem. Phys.* **2012**, *137* (24), 241101.
(31) Xiong, B.; Chang, Y.-C.; Ng, C.-Y. A Quantum-Rovibrational-State-Selected Study of the Proton-Transfer Reaction $H_2^+(X^2\Sigma_g^+: v^+ = 1-3; N^+ = 0-3)$ + Ne → NeH+ + H Using the Pulsed Field Ionization-Photoion Method: Observation of the Rotational Effect near the Reaction Threshold. *Phys. Chem. Chem. Phys.* **2017**, *19* (28), 18619−18627.
(32) Xiong, B.; Chang, Y.-C.; Ng, C.-Y. Quantum-State-Selected Integral Cross Sections for the Charge Transfer Collision of O2+(a4[capital Pi]u5/2,3/2,1/2,-1/2: ν+ = 1−2; J+) [O2+(X2-[capital Pi]g3/2,1/2: ν+ = 22−23; J+)] + Ar at Center-of-Mass Collision Energies of 0.05−10.00 eV. *Phys. Chem. Chem. Phys.* **2017**, *19* (43), 29057−29067.
(33) Xu, Y.; Xiong, B.; Chang, Y. C.; Ng, C. Y. The Translational, Rotational, and Vibrational Energy Effects on the Chemical Reactivity of Water Cation $H_2O^+(X^2B_1)$ in the Collision with Deuterium Molecule D_2. *J. Chem. Phys.* **2013**, *139*, 024203.
(34) Song, H.; Li, A.; Guo, H.; Xu, Y.; Xiong, B.; Chang, Y.-C.; Ng, C. Comparison of Experimental and Theoretical Quantum-State-Selected Integral Cross-Sections for the $H_2O^+ + H_2(D_2)$ Reactions in the Collision Energy Range of 0.04−10.00 eV. *Phys. Chem. Chem. Phys.* **2016**, *18* (32), 22509−22515.
(35) Xu, Y.; Xiong, B.; Chang, Y. C.; Ng, C. Y. Isotopic and Quantum-Rovibrational-State Effects for the Ion−Molecule Reaction $H_2O^+(X^2B_1: v_1^+v_2^+v_3^+; N^+Ka+Kc+)$ + HD in the Collision Energy Range of 0.03−10.00 eV. *Phys. Chem. Chem. Phys.* **2017**, *19* (13), 8694−8705.
(36) Xu, Y.; Xiong, B.; Chang, Y.-C.; Pan, Y.; Lo, P. K.; Lau, K. C.; Ng, C. A Quantum-Rovibrational-State-Selected Study of the $H_2O^+(X^2B_1: v_1^+v_2^+v_3^+; N^+Ka+Kc+)$ + CO Reaction in the Collision Energy Range of 0.05−10.00 eV: Translational, Rotational, and vibrational energy effects. *Phys. Chem. Chem. Phys.* **2017**, *19* (15), 9778−9789.
(37) Li, A.; Li, Y.; Guo, H.; Lau, K.-C.; Xu, Y.; Xiong, B.; Chang, Y.-C.; Ng, C. Y. Communication: The origin of Rotational Enhancement Effect for the Reaction of $H_2O^+ + H_2$ (D_2). *J. Chem. Phys.* **2014**, *140* (1), 011102.
(38) Ard, S. G.; Li, A.; Martinez, O.; Shuman, N. S.; Viggiano, A. A.; Guo, H. Experimental and Theoretical Kinetics for the $H_2O^+ + H_2/D_2 \rightarrow H_3O^+/H_2DO^+ + H/D$ Reactions: Observation of the Rotational

DOI: 10.1021/acs.jpca.8b04587
J. Phys. Chem. A 2018, 122, 6491−6499

Effect in the Temperature Dependence. *J. Phys. Chem. A* **2014**, *118* (49), 11485−11489.
(39) Lavvas, P.; Yelle, R.; Heays, A.; Campbell, L.; Brunger, M.; Galand, M.; Vuitton, V. N_2 State Population in Titan's Atmosphere. *Icarus* **2015**, *260*, 29−59.
(40) Song, H.; Li, A.; Yang, M.; Guo, H. Competition between the H-and D-Atom Transfer Channels in the H_2O^+ + HD Reaction: Reduced-Dimensional Quantum and Quasi-Classical Studies. *Phys. Chem. Chem. Phys.* **2017**, *19*, 17396.
(41) Chantry, P. J. Doppler Broadening in Beam Experiments. *J. Chem. Phys.* **1971**, *55* (6), 2746−2759.
(42) Ruscic, B.; Feller, D.; Peterson, K. A. Active Thermochemical Tables: Dissociation Energies of Several Homonuclear First-Row Diatomics and Related Thermochemical Values. *Theor. Chem. Acc.* **2014**, *133* (1), 1415.
(43) Pollard, J. E.; Trevor, D. J.; Reutt, J. E.; Lee, Y. T.; Shirley, D. A. Torsional Potential and Intramolecular Dynamics in the $C_2H_4^+$ Photoelectron Spectra. *J. Chem. Phys.* **1984**, *81* (12), 5302−5309.
(44) Kim, M. H.; Leskiw, B. D.; Suits, A. G. Vibrationally Mediated Photodissociation of Ethylene Cation by Reflectron Multimass Velocity Map Imaging. *J. Phys. Chem. A* **2005**, *109* (35), 7839−7842.
(45) Weitzel, K.-M.; Jarvis, G.; Malow, M.; Baer, T.; Song, Y.; Ng, C. Observation of Accurate Ion Dissociation Thresholds in Pulsed Field Ionization-Photoelectron Studies. *Phys. Rev. Lett.* **2001**, *86* (16), 3526.
(46) Lias, S. G.; Bartmess, J. E.; Liebman, J. F.; Holmes, J. L.; Levin, R. D.; Mallard, W. G. Gas-Phase Ion and Neutral Thermochemistry. *Journal of Physical and Chemical Reference Data, Supplement No. 1*; 1988; Vol. *17*.
(47) Gioumousis, G.; Stevenson, D. P. Reactions of Gaseous Molecule Ions with Gaseous Molecules. V. Theory. *J. Chem. Phys.* **1958**, *29* (2), 294−299.
(48) Bose, T. K.; Cole, R. H. Dielectric and Pressure Virial Coefficients of Imperfect Gases. IV C_2H_4 and C_2H_4−Ar Mixtures. *J. Chem. Phys.* **1971**, *54* (9), 3829−3833.
(49) Kimura, K. *Handbook of HeI Photoelectron Spectra of Fundamental Organic Molecules: Ionization Energies, ab initio Assignments, and Valence Electronic Structure for 200 Molecules*; Japan Scientific Societies Press, 1981.
(50) Stockbauer, R.; Inghram, M. G. Threshold Photoelectron−Photoion Coincidence Mass Spectrometric Study of Ethylene and Ethylene-d4. *J. Chem. Phys.* **1975**, *62* (12), 4862−4870.
(51) Bombach, R.; Dannacher, J.; Stadelmann, J.-P. The Rate/Energy Functions for the Competitive Fragmentation Processes of Ethylene and Ethane Cations. *Int. J. Mass Spectrom. Ion Processes* **1984**, *58*, 217−231.

DOI: 10.1021/acs.jpca.8b04587
J. Phys. Chem. A 2018, 122, 6491−6499